AGU PUBLICATIONS

Global Biogeochemical Cycles

RESEARCH ARTICLE
10.1002/2013GB004754

Key Points:
- Multi-proxy record of nutrient loading in long-lived deep-sea corals
- Bulk and compound-specific isotopes capture changes in watershed quality
- Novel approach to coupled tracer of agro-industrialization and land-use changee

Correspondence to:
N. G. Prouty,
nprouty@usgs.gov

Citation:
Prouty, N. G., E. B. Roark, A. E. Koenig, A. W. J. Demopoulos, F. C. Batista, B. D. Kocar, D. Selby, M. D. McCarthy, F. Mienis, and S. W. Ross (2014), Deep-sea coral record of human impact on watershed quality in the Mississippi River Basin, *Global Biogeochem. Cycles*, *28*, 29–43, doi:10.1002/2013GB004754.

Received 17 OCT 2013
Accepted 20 DEC 2013
Accepted article online 4 JAN 2014
Published online 27 JAN 2014
Corrected 11 MAY 2014

This article was corrected on 11 MAY 2014. See the end of the full text for details.

Deep-sea coral record of human impact on watershed quality in the Mississippi River Basin

Nancy G. Prouty[1], E. Brendan Roark[2], Alan E. Koenig[3], Amanda W.J. Demopoulos[4], Fabian C. Batista[5], Benjamin D. Kocar[6], David Selby[7], Matthew D. McCarthy[5], Furu Mienis[8], and Steve W. Ross[9]

[1]US Geological Survey, Santa Cruz, California, USA, [2]Department of Geography, Texas A&M University, College Station, Texas, USA, [3]US Geological Survey, Denver, Colorado, USA, [4]US Geological Survey, Gainesville, Florida, USA, [5]University of California, Santa Cruz Ocean Sciences Department, Santa Cruz, California, USA, [6]Stanford Synchrotron Radiation Lightsource, Menlo Park, California, USA, [7]Department of Earth Science, Durham University, Durham, UK, [8]Royal Netherlands Institute for Sea Research, Texel, Netherlands, [9]Center for Marine Science, University of North Carolina Wilmington, Wilmington, North Carolina, USA

Abstract One of the greatest drivers of historical nutrient and sediment transport into the Gulf of Mexico is the unprecedented scale and intensity of land use change in the Mississippi River Basin. These landscape changes are linked to enhanced fluxes of carbon and nitrogen pollution from the Mississippi River, and persistent eutrophication and hypoxia in the northern Gulf of Mexico. Increased terrestrial runoff is one hypothesis for recent enrichment in bulk nitrogen isotope ($\delta^{15}N$) values, a tracer for nutrient source, observed in a Gulf of Mexico deep-sea coral record. However, unambiguously linking anthropogenic land use change to whole scale shifts in downstream Gulf of Mexico biogeochemical cycles is difficult. Here we present a novel approach, coupling a new tracer of agro-industrialization to a multiproxy record of nutrient loading in long-lived deep-sea corals collected in the Gulf of Mexico. We found that coral bulk $\delta^{15}N$ values are enriched over the last 150–200 years relative to the last millennia, and compound-specific amino acid $\delta^{15}N$ data indicate a strong increase in baseline $\delta^{15}N$ of nitrate as the primary cause. Coral rhenium (Re) values are also strongly elevated during this period, suggesting that 34% of Re is of anthropogenic origin, consistent with Re enrichment in major world rivers. However, there are no pre-anthropogenic measurements of Re to confirm this observation. For the first time, an unprecedented record of natural and anthropogenic Re variability is documented through coral Re records. Taken together, these novel proxies link upstream changes in water quality to impacts on the deep-sea coral ecosystem.

1. Introduction

Deep-sea corals incorporate the geochemical signature of recently exported matter into their skeletons. Analogous to sediment trap records, proteinaceous deep-sea corals that build their skeleton out of organic material have the potential to record changes in nutrient fluxes over decadal to century time scales [*Williams et al.*, 2007; *Williams and Grottoli*, 2010a, 2010b; *Sherwood et al.*, 2011]. In particular, proteinaceous collected on continental shelves are presumably sensitive to changes in nutrient fluxes associated with terrestrial runoff, potentially integrating watershed changes from nearby drainage basins. Several studies have documented the sensitivity of shallow proteinaceous corals (e.g., black and gorgonin corals) to land-based nutrient input, linking the skeletal bulk nitrogen isotope ($\delta^{15}N$) values, a tracer for nutrient source, to changes in terrestrial pollution [*Risk et al.*, 2009; *Sherwood et al.*, 2010; *Baker et al.*, 2010]. Increased terrestrial runoff is also one hypothesis for recent enrichment in skeletal $\delta^{15}N$ observed in a deep-sea black coral record from the Gulf of Mexico [*Williams et al.*, 2007]. Because proteinaceous corals feed primarily on exported sinking particles [*Roark et al.*, 2009], long-lived deep-sea black corals living adjacent to watersheds are potentially linked to river discharge. The Mississippi River is the third largest river basin in the world and accounts for 90% of the freshwater inflow to the Gulf of Mexico, dispersing large amounts of terrestrial organic matter and nutrients. The resulting high level of primary productivity produces marine organic matter that sinks to the seafloor [*Mienis et al.*, 2012]. Unlike sediment traps, deep-sea black corals provide detailed records over the centennial- to millennial-scale lifespans of individual colonies [*Roark et al.*, 2009], placing recent biogeochemical change into a tightly constrained temporal perspective linked to watershed land use changes. In the Mississippi River Basin, these landscape changes are linked to enhanced fluxes of carbon and nitrogen pollution from the Mississippi River [*McIsaac et al.*, 2001; *Raymond et al.*, 2008], and persistent eutrophication and hypoxia in the northern Gulf of Mexico [*Rabalais et al.*, 2002].

Scavenging of terrestrially derived metals by marine biota represents an important pathway from the coastal land-sea interface to the deep sea [*Morel and Price*, 2003]. This is especially true for elements that are highly mobile in biogeochemical cycles. Rhenium (Re), in particular, is highly susceptible to anthropogenic mobilization (e.g., fossil fuel combustion, mining, and biomass burning) relative to natural mobilization (e.g., sea salt aerosol emissions, sediment denudation, and net primary productivity) [*Klee and Graedel*, 2004]. Because of its high mobility, Re released to the environment can be easily leached from ash fallout or mine tailings [*Miller et al*., 2011] and carried to rivers [*Colodner et al*., 1993; *Rahaman et al*., 2012]. However, little is known about the behavior of Re in the marine system. Marine chemistry of Re is of interest due to its extreme enrichment in reducing sediments compared to oxic sediments [e.g., *Crusius et al*., 1996], utility for dating ancient sedimentary rocks using the Re-Os (Osmium) geochronometer [e.g., *Selby and Creaser*, 2005] and role as a chemical analog for technetium-99 (^{99}Tc), a by-product of nuclear fuel reprocessing and nuclear explosion tests [*Wakoff and Nagy*, 2004]. Given its high mobility and diagnostic sources, Re can be used to understand erosion, weathering, and the carbon cycle [*Peucker-Ehrenbrink and Ravizza*, 2000]. The tightly coupled surface cycles of Re and organic carbon (C_{org}) provide a tool to calculate CO_2 flux because the weathering of organic-rich sediments is their common source [*Dalai et al*., 2002; *Jaffe et al*., 2002]. However, recent examination of Re concentrations in major rivers worldwide suggests that observed Re enrichment is largely due to human activity, with 32% of Re anthropogenically sourced [*Miller et al*., 2011]. However, to date there are no pre-anthropogenic measurements of Re that can be used to validate this hypothesis. Rhenium values in deep-sea coral skeletons, when coupled with stable isotope records, may represent a powerful new approach for simultaneous assessment of downstream effects on ocean biogeochemical cycles. Here we present a novel approach, coupling a new tracer of agro-industrialization to a multiproxy record of nutrient loading in long-lived deep-sea corals collected in the Gulf of Mexico. Measurements of trace metals, bulk nitrogen (δ^{15}N), and compound-specific amino acid δ^{15}N (δ^{15}N-AA) isotopes capture the rapid sensitivity of deep-sea corals to upstream changes in watershed quality linked to the onset of agro-industrialization and the intensity of land use change. Results from this novel approach not only provide a temporal perspective over the last millennia, but also a quantitative context to evaluate effects of future and ongoing land use and climate change on nutrient loading and marine ecosystem health.

2. Materials and Methods

2.1. Sample Site and Coral Collection

Deep-sea coral specimens for this study were collected east of the Mississippi Delta in the Gulf of Mexico between 2003 and 2009 at the head of De Soto Canyon and in the Viosca Knoll (VK) region (Figure 1 and Table 1) as part of several ongoing deep-sea coral ecosystem studies [*CSA International*, 2007; *Sulak et al*., 2008]. Sediment trap studies at Viosca Knoll highlight the dominance of the Mississippi-Atchafalaya River as the source of sediment and nutrient transport to the seafloor of this region [*Davies et al*., 2010; *Mienis et al*., 2012]. Near bed measurements reported in *Mienis et al*. [2012] showed peaks in fluorescence, which are related to surface blooms, and peaks in fluorescence correspond to increased levels of pigments, organic carbon (C_{org}), total nitrogen (N_{tot}), and biogenic silica (SiO_2) in the sediment trap, representing an important source of nutrition in the Viosca Knoll coral area. The manned submersible, Johnson-Sea-Link (JSL, Harbor Branch Oceanographic Institute), was used to collect live black coral colonies from the Viosca Knoll (VK) sites at depths of 310–317 m (Table 1). A bottom trawl inadvertently collected specimens of living black coral from the head of De Soto Canyon at a depth of 304 m (Figure 1). Black coral specimens from the De Soto Canyon were tentatively identified based on branch pattern and size as *Leiopathes* sp.; remaining samples were identified at the time of collection and confirmed by comparisons with previously identified black corals.

2.1.1. Chronology

Cross-sectional disks ~0.3 to 0.5 cm thick were cut from the basal portion of the corals using a diamond band saw and prepared for geochemical analysis (i.e., stable, radio-isotopes, and trace metals). Discrete samples were separated by placing the disks, consisting primarily of chitin and protein [*Goldberg*, 1991], in a solution of 4 g of potassium hydroxide (KOH) in 50 mL of water for ~1 week [*Williams et al*., 2006, 2007]. The KOH acts as an effective protein denaturant and solvent causing the skeleton to swell and growth laminae to separate. This treatment does not appear to have any effect on the stable or radio isotopic composition of the skeleton [*Williams et al*., 2007; *Prouty et al*., 2011]. Using forceps and a light microscope, individual bands were separated, rinsed with Milli-Q water, and dried overnight. Individual growth laminae were used for radiocarbon dating, stable

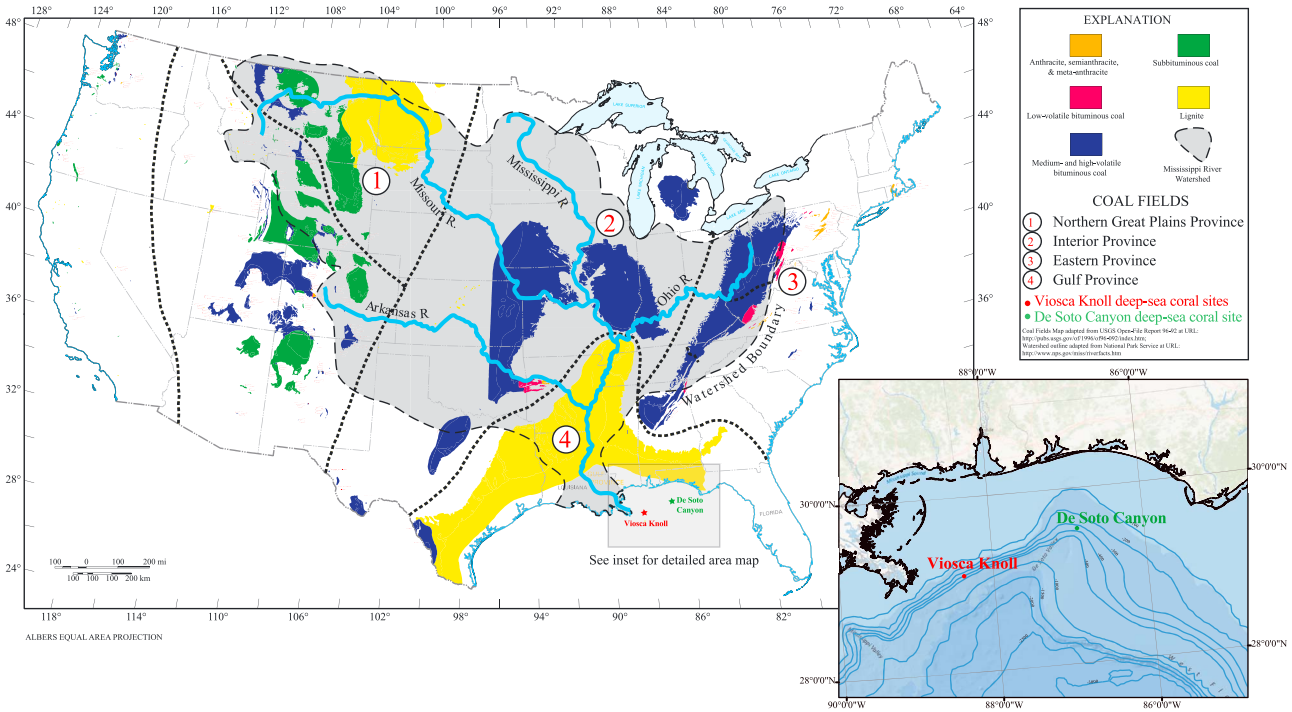

Figure 1. Deep-sea coral samples (Leiopathes sp.) for this study were collected between 2003 and 2009 from two different sites on the upper De Soto Slope subprovince, the head of De Soto Canyon and Viosca Knoll (VK). Both a trawl net and a manned submersible, Johnson-Sea-Link, were used to collect samples at water depths of approximately 300 m (inset). The four major coal-producing regions are shown in relation to the areal extent of the Mississippi River watershed.

isotope, and trace element analyses, all detailed below. Coral samples were dated using previously established radiocarbon (^{14}C) methods that provide robust and reliable chronologies for black corals [*Roark et al.*, 2009]. Radiocarbon derived chronologies for the black corals analyzed here are reported in *Prouty et al.* [2011] and were used for the stable isotopic (bulk and compound specific) time series and Re concentration maps by converting the measured variable versus radial distance to measured variable versus age by applying the radial growth rates and linear-age models. Results from the radiocarbon analysis of the oldest *Leiopathes* sp. specimen from this region at 300 m water depth indicate that these animals have been growing continuously for at least the last two millennia, with radial growth rates ranging from 8 to 22 μm yr^{-1} as reported in *Prouty et al.* [2011].

2.2. Rhenium Coral Analysis

Newly developed Laser Ablation Inductively Coupled Mass Spectrometry (LA-ICP-MS) methods were used to measure Re variability using a 193 nm wavelength laser connected to an Elan DRC-e quadrupole ICP-MS at the United States Geological Survey (USGS) LA-ICP-MS Facility in Denver, CO, following methods for quantitative trace element mapping [*Koenig et al.*, 2009]. A prototype reference material with a similar organic matrix as the black corals was developed for this work that consisted of a combination of trace elements in oil and organometallic compounds added to an epoxy base. The new standard was characterized for the trace

Table 1. Sample ID and Location for *Leiopathes* sp. Specimens Collected Between 2003 and 2009 Within the Gulf of Mexico From Two Different Sites on the Upper De Soto Slope Subprovince, the Head of De Soto Canyon (Archived at the US National Museum, U.S.N.M.) and Viosca Knoll (VK)[a]

Sample ID	Collection Date	Site	Lat.	Long.	Depth (m)
GOM-TOW-BC1	11/15/03	De Soto Canyon	29°32.24′N	86°52.19′W	304
GOM-TOW-BC2	11/15/03	De Soto Canyon	29°32.24′N	86°52.19′W	304
GOM-JSL05-4876-BC1	9/17/05	VK 906/907	29°06.25′N	88°23.5′W	312
GOM-JSL09-3728-BC1	9/20/09	VK 862	29°06.41′N	88° 23.10′W	317
GOM-JSL04-4734-BC1	7/23/04	VK 862	29°06.22′N	88°23.05′W	310

[a]Samples IDs include information about whether the samples were collected by trawl (TOW) or manned submersible, Johnson-Sea-Link (JSL).

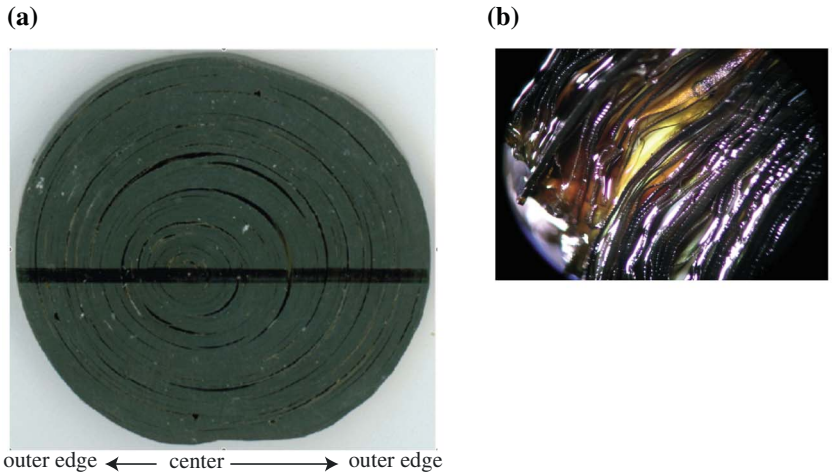

Figure 2. (a) Image of coral disc showing laser transect across the diameter (~2.7 cm) of the black coral specimen (GOM-JSL09-3728-BC1). (b) Petrographic image (27 mm × 46 mm) illustrating skeletal microlayers (image courtesy of N. Buster).

element concentrations by solution ICP-MS and instrumental neutron activation analysis (INAA) and used as one of the internal standards to convert individual intensity (CPS) measurements to concentration values, parts per million (ppm). The LA-ICP-MS quantification was conducted using a modified procedure, with each time slice along the line scan treated as an individual measurement and converted to concentration [*Longerich et al.*, 1996]. To account for differences in yield, elemental concentrations were normalized to a constant percent carbon (45%). Total organic carbon (TOC) concentrations were determined by a UIC Coulometrics CM5012 CO_2 coulometer via combustion at the USGS Laboratories in Santa Cruz, CA, and %C results were confirmed by elemental analysis from the Stable Isotope Geosciences Facility at Texas A&M. A pre-ablation cleaning scan was run prior to collecting data. In order to produce a rectangular elemental concentration map, a series of stacked radial lines (between 20 and 40) spaced ~40 μm apart were scanned at 20 μm s^{-1} scan speed using a 35 μm spot size across the entire diameter of the specimen (Figure 2a). The LA-ICP-MS quantification was conducted using a procedure where each time slice along the line scan was treated as an individual intensity (CPS) measurement and converted to concentration values (ppm) based on calibrations using international and internal standards. Time slices were converted to X-Y grid and a Krigging algorithm was used to produce the concentration maps. For signal verification, trace metal analyses for Re variability were also performed on discrete growth layers using solution ICP-MS.

2.3. Rhenium Speciation: XANES Spectroscopy

The spatial Re distribution and speciation were determined using high-resolution (2 μm diameter beam) X-ray fluorescence (XRF) mapping and X-ray absorption spectroscopy (XAS) at the Stanford Synchrotron Radiation Lightsource (SSRL), using the hard X-ray microprobe (beamline 2–3). A Si(111) crystal set was used for energy selection, and X-ray fluorescence was measured using a single-element Vortex detector. X-ray fluorescence mapping was performed at 12,000 eV, above the Re L_{III} edge of 10,535 eV, using a step size of 5 μm and a dwell time of 25 ms. Using the fluorescence map as a guide, two points—one at the core of the coral sample (oldest portion) and another at the outer edge (youngest portion)—were chosen to examine the speciation of Re using X-ray absorption near edge structure (XANES) spectroscopy. XANES spectra were collected from ~ −231 eV to ~214 eV relative to the Re L_{III} edge, with short (0.35 eV) steps taken across the absorption edge (~10,500–10,570 eV). Five and six XANES spectra were collected at each point, respectively —individual spectra were then averaged for each point. Energy calibration was achieved by scanning a Re(0) foil and setting the resulting first derivative inflection point to 10,535 eV. Spectra were compared to the standard foil, as well as a dilute Re(VII) oxide (Re_2O_7) standard.

2.4. Rhenium Analysis in Sediment, Macroalgae, and Zooplankton Samples

As a potential contributor to detrital organic matter and food to the benthic community [*Schoener and Rowe*, 1970], as well as a bio-accumulator of Re [*Scadden*, 1969; *Yang*, 1991; *Mas et al.*, 2005], individual brown algae

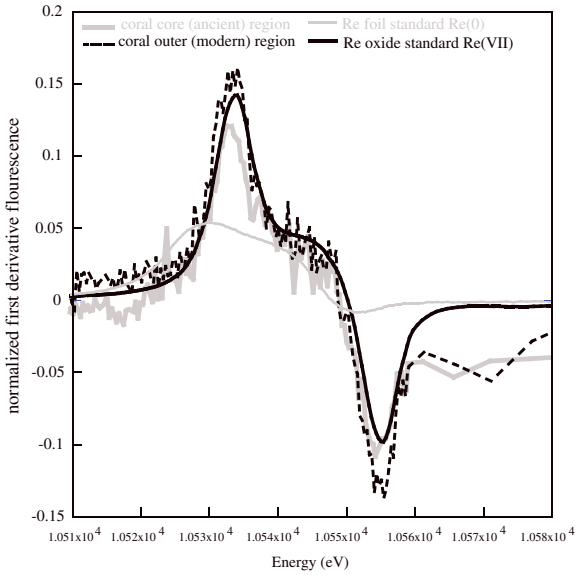

Figure 3. The first derivative of LIII-edge X-ray absorption spectra derived from a Re foil standard Re(0) and a Re(VII) oxide (Re2O7) standard relative to the absorption spectra from both the core region (oldest) and the outer edge region (youngest) of the black coral sample (GOM-JSL09-3728-BC1). Absorption spectra for the black corals represent the average of five and six individual XANES scans at the core and outer region, respectively.

samples (*Sargassum fluitans* and *Sargassum natans*) collected from surface waters in the Gulf of Mexico (collections were between 26 and 28°N and 87 and 89°W) were analyzed for Re. Zooplankton samples were also collected from the sediment trap samples, and surface particulate organic matter (POM) was collected at sea between 2007 and 2010 in the VK826 region by filtering 7–10 L of surface seawater through a 47 mm 0.40 μm GFF. *Sargassum* samples were kept frozen until sample pretreatment, which included rinsing with de-ionized (DI) water 3× to remove any epibiota, rinsing in 10% HCl, sonicating, rinsing again in DI, and drying overnight at 40°C. Rhenium was analyzed by solution ICP-MS at USGS Mass Spectrometry Facilities in Denver, CO, which included ashing up to 5 g of sample overnight at 450°C and then digesting the residue using a 4-acid procedure (HF + HCl + HNO3 + $HClO_4$). Three samples were also analyzed at Durham University utilizing the same method described for coal samples below. Filters for zooplankton were freeze dried upon collection, and zooplankton material was scrapped off for analysis by solution ICP-MS using a 4-acid procedure described above. The POM filters including blanks were dried at 50°C and acidified with 1N HCl. The POM and filter were digested using a 4-acid procedure, using 4 mL of HF in order to dissolve the filter matrix for solution ICP-MS analysis. Sediment samples from the top section (0–2 cm) of tube cores collected in 2009–2010 from Viosca Knoll lease blocks 826, 862, and 906 at an average depth of 450 m and monthly sediment trap samples collected in 2009–2010 from VK826 at a depth of 480 m were analyzed for Re composition by ICP-MS and ICP-OES at Bremen University, the Royal Netherlands Institute for Sea Research, and USGS (Denver, CO). In brief, between 50 and 100 mg were digested using a 4-acid procedure, taken to dryness, and residue dissolved in 5–20 mL of 5–13% HNO_3 with a dilution factor of 10^3 to 10^4.

2.5. Quantification of Rhenium in Coal Samples

Coal samples were chosen for Re analysis within the Mississippi River watershed, encompassing two of the major coal producing regions (Interior and Gulf Provinces) of the US (Figure 1). Coal samples were obtained commercially from Ashbury Graphite Mills and the Department of Penn State Coal Sample Bank and Data Base and were analyzed for Re using Carius tube isotope dilution negative thermal ionization mass spectrometry at the University of Arizona and Durham University. Approximately 100–200 mg of powder was digested with a known amount of ^{185}Re in 1:3 mix of HCl-HNO_3 (9 mL) in a Carius tube at 220°C for 48 h. The Re was purified from the acid solution using standard anion chromatography methods, with the Re fraction measured by negative thermal mass spectrometry [*Selby and Creaser*, 2001; *Kirk et al*., 2002].

2.6. Bulk and Compound-specific Stable Isotope Analysis

Carbon ($\delta^{13}C$) and nitrogen ($\delta^{15}N$) stable isotope analyses were performed on discrete subsamples of black coral skeleton material and black coral tissue. Growth laminae were identified using a reflected-light microscope. The presences of individual growth bands were evident on scanning electron microscope (SEM) images illustrated in *Prouty et al*. [2011]. As described in *Prouty et al*. [2011], growth bands, which may consist of more than one individual (e.g., annual) layer (Figure 2b), were separated using forceps and a reflected-light microscope. Individual growth lamine were less than 100 μm thick except in the core region of each specimen where typical thickness of growth layers was between 250 and 350 μm. Bulk stable isotope analysis was performed using a Delta Plus XL with a Carlo Erba Elemental analyzer at the Stable Isotope Geosciences Facility at Texas A&M where ~500 μg of black coral skeleton material was analyzed

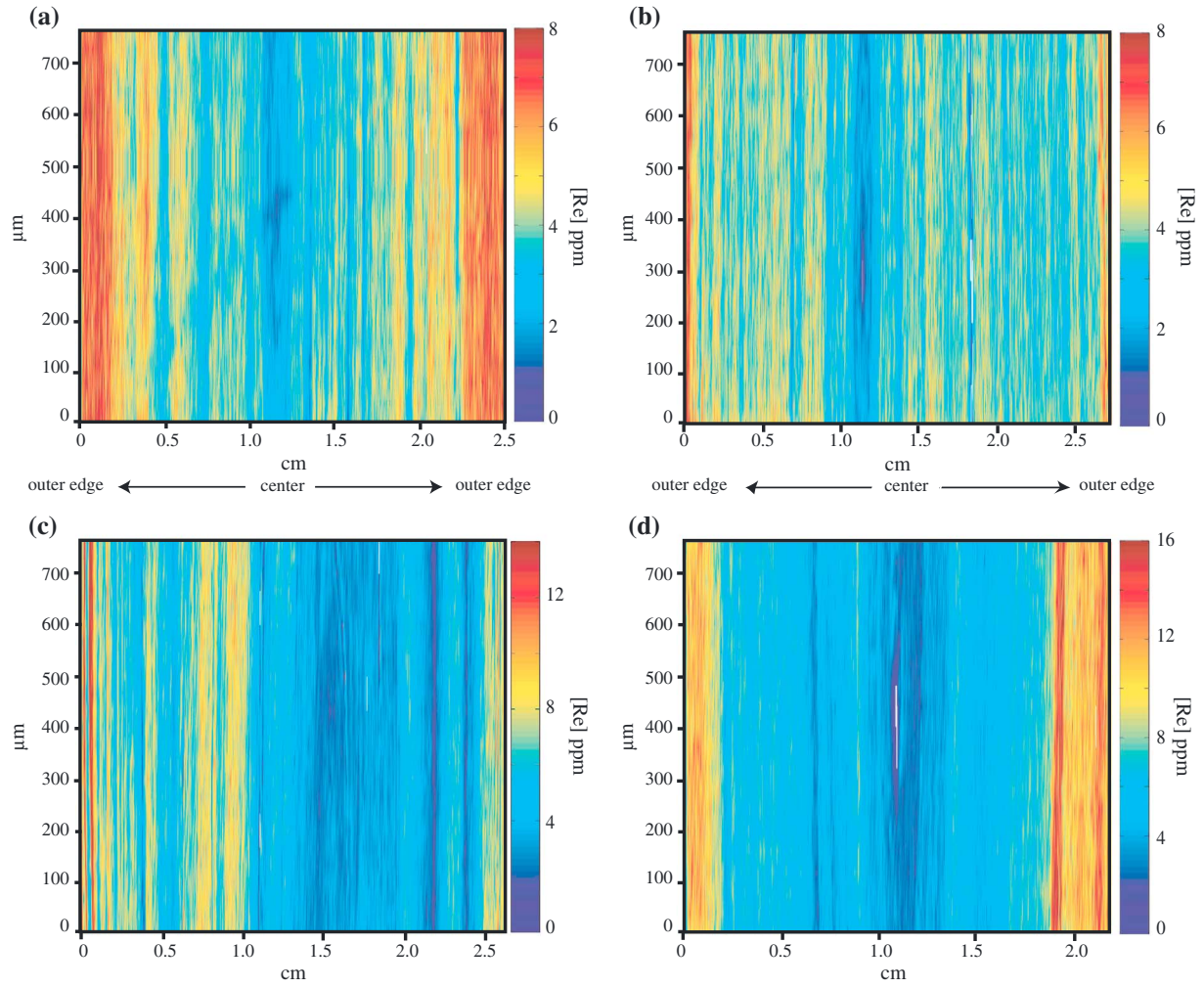

Figure 4. Rhenium (Re) concentration versus distance maps were constructed from laser ablation inductively coupled mass spectrometry (LA-ICPMS) methods. Black corals discs were ablated across the radial transect using a 35 µm spot size to scan 20 lines spaced 40 µm apart across the entire diameter (outer edge to center to outer edge) of each specimen. Intensity (CPS) was converted to ppm based on calibrations using international and internal standards and converted to X-Y grid and Krigging algorithm to produce the concentration maps ((a) GOM-TOW-BC2, (b) GOMJSL09-3728-BC1, (c) GOM-JSL05-4876-BC1, and (d) GOM-JSL04-4734-BC1).

per growth band, as defined above. Analyses were made and calibrated against internal laboratory standards and international standards. Results are reported in conventional per mil (‰) notation relative to VPDB ($\delta^{13}C$) and air ($\delta^{15}N$). Reproducibility of the isotope results is ±0.15‰ for both $\delta^{13}C$ and $\delta^{15}N$ based international and internal standards. Replicate analyses of corals samples also fall within or near to the analytical reproducibility range with an average difference between replicated layers of 0.22 ‰ ($n = 21$) for $\delta^{15}N$ and 0.36 ‰ ($n = 21$) for $\delta^{13}C$.

Individual $\delta^{15}N$-AA analysis was made on acid hydrolysates (6 N HCl, 100 mL, 20 h) following formation of isopropyl-TFA derivatives [*McCarthy et al.*, 2007; *Sherwood et al.*, 2011] of approximately 5–30 mg of black coral skeleton from 13 discrete growth layers from the coral sample GOM-JSL09-3728-BC1. Samples GoM 1.2–1.9 were derived from the outermost 320 µm at approximately 35 µm increments and represent skeletal growth from 2003 to 1965 AD assuming a growth rate of 8 µm yr^{-1} [*Prouty et al.*, 2011]. Samples GoM 7.5–7.9 were sampled between 13.23 and 14.27 mm radial distance from the outer edge at approximately 350 µm intervals and represent skeletal growth centered at 290 AD.

Derivatives were analyzed on a thermo Trace Ultra GC, fitted with an SGE BPX5 column, in line with an oxidation furnace and reduction furnace, and linked to a Finnigan Delta^{plus} XP mass spectrometer at the University of California, Santa Cruz. Samples were injected in triplicate, bracketed by standards, and sample

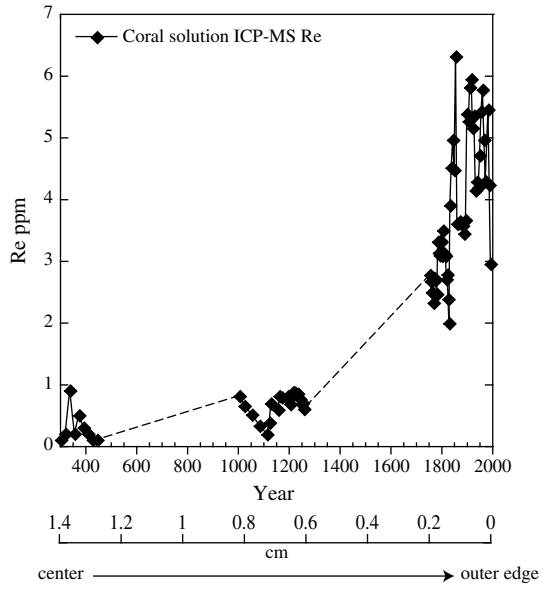

Figure 5. Trace metal analysis for rhenium (Re) concentration was performed on discrete growth layers using solution ICP-MS. In the outer, mid, and center regions of the radial transect, samples were taken at intervals of approximately 39, 97, and 143 μm, respectively. Rhenium concentrations were elevated in the outermost region of the sample (GOM-JSL09-3728-BC1), consistent with the laser results (Figure 4).

$\delta^{15}N$ values were corrected based on standard values. Reproducibility for individual amino acid (AA) values was typically better than 1‰. Values for $\delta^{15}N$ were measured for alanine (Ala), aspartic acid + asparagine (Asp), glutamic acid + glutamine (Glu), isoleucine (Ile), leucine (Leu), proline (Pro), valine (Val), glycine (Gly), lysine (Lys), phenylalanine (Phe), serine (Ser), threonine (Thr), and tyrosine (Tyr). Trophic position (TP) was calculated as $TP_{Glu/Phe} = (\delta^{15}N_{Glu} - \delta^{15}N_{Phe} - 3.4‰)/7.6‰ + 1$ [*Chikaraishi et al.*, 2009].

3. Results

3.1. Coral Rhenium Concentration and Speciation

The dominant form of Re in seawater is perrhenate anion, ReO_4^- (Re(VII)), which is highly soluble and readily bioavailable [*Tagami and Uchida*, 2008]. In contrast, Re in reducing sediments is typically found as $Re(OH)_4$ [*Crusius et al.*, 1996]. The first derivative of K-edge X-ray absorption spectra derived from a Re foil standard Re(0) and a Re(VII) oxide (Re_2O_7) standard was compared to the absorption spectra of the black coral. The absorption spectra of both the oldest portion and youngest portion of coral growth match the absorption spectra of the Re oxide standard (Figure 3), indicating that uptake of Re by black corals is in the form of highly soluble and stable perrhenate anion ReO_4^- (Re(VII)) rather than the reduced form, $Re(OH)_4$.

Rhenium concentrations, as determined by LA-ICP-MS from black coral specimens collected in the Gulf of Mexico, range between less than 1 ppm within the core region to over 14 ppm in the outermost portion of skeletal growth (Figure 4). This pattern was also observed in the solution ICP-MS results (Figure 5). The Re pattern observed in all the specimens shows a marked rise during the last 150–200 years (Figure 6). According to the growth rate estimates [*Prouty et al.*, 2011], the Re increase near Viosca Knoll began in the late 1800s, and the De Soto Canyon specimen suggests that Re increased slightly earlier, starting in the early to mid-1800s (Figure 6).

To back calculate pre-anthropogenic Mississippi River seawater and freshwater end-member Re concentrations, a concentration factor (CF) was calculated from the present-day average seawater end-member value, 8.3 parts per trillion (ppt) [*Miller et al.*, 2011; *Shim et al.*, 2012], and the average present-day coral Re value at Viosca Knoll, 8–9 parts per million (ppm) (this study), yielding a CF of 10^6 (Table 2). Using the slope of conservative mixing line (-2×10^{-7}; Table 2) and coral Re values prior to the 19th century increase (~4 ppm), the CF yields a pre-anthropogenic Mississippi River seawater and freshwater end-member Re concentration of approximately 3.9 and 10.8 ppt, respectively (Table 2). Comparing the present-day freshwater end-member Re value, 16.5 ppt, to estimated pre-anthropogenic freshwater end-member Re value, 10.8 ppt, yields an anthropogenic contribution of approximately 34% to present-day Mississippi River freshwater end-member Re concentrations (Table 2).

3.2. Rhenium Inventory: POM, Zooplankton, and Sediment

The surface POM Re values average 0.3 ± 0.27 ppt with a range of 0.005 to 1.6 ppt (Table 3). The monthly zooplankton samples yield a Re range between 0.2 and 1.4 ppt with an average concentration of 0.7 ± 0.38 ppt, with peak values in May corresponding to peak Mississippi-Atchafalaya river discharge [*Aulenbach et al.*, 2007] (Figure 7). *Sargassum* spp. samples from the Gulf of Mexico contained Re at concentrations of less than 1 part per billion (ppb) (Table 3), significantly less compared to other brown algae species from the Pacific and Atlantic

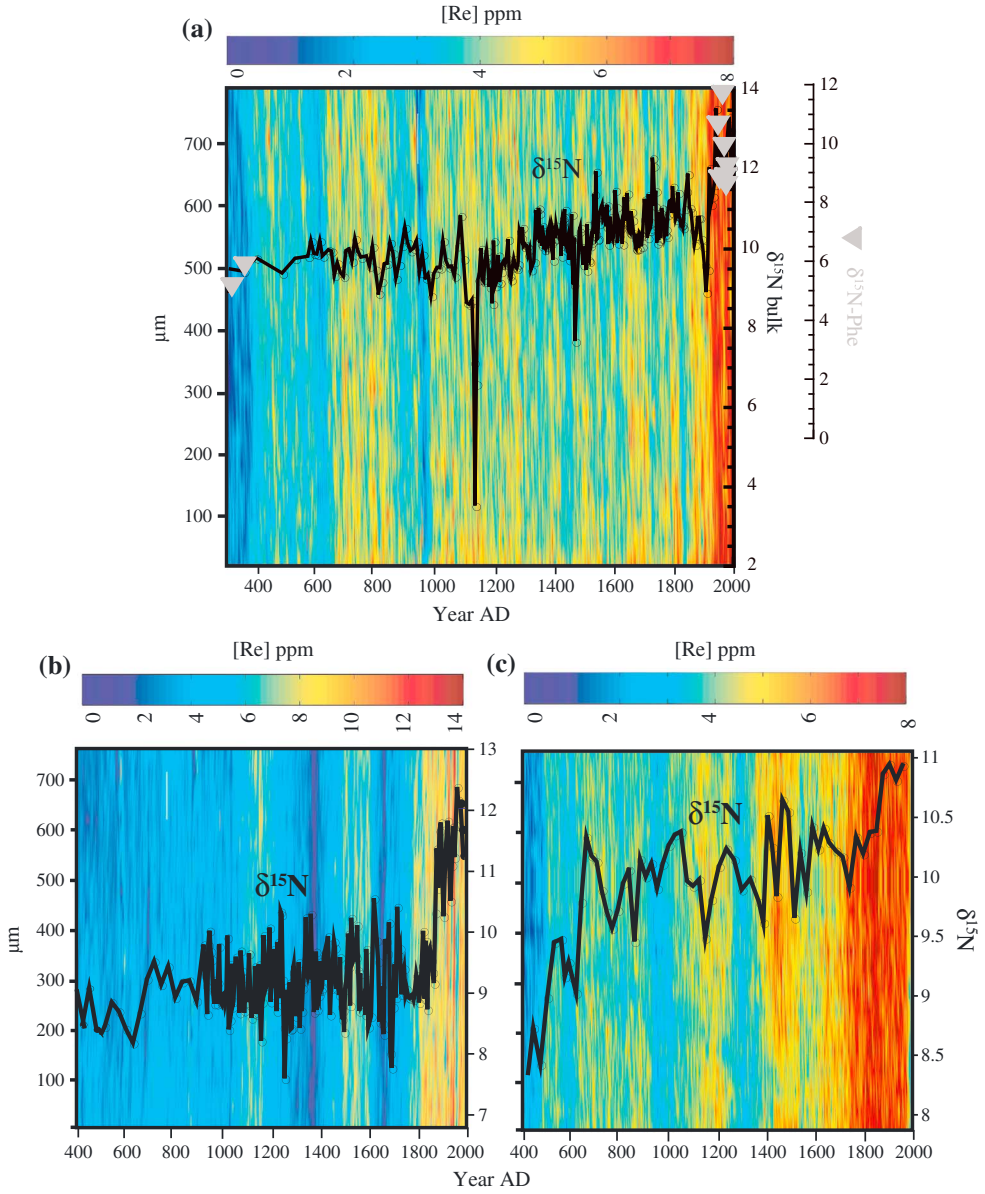

Figure 6. Concentration maps demonstrate rhenium (Re) enrichment both spatially within the corals' microstructure as well as temporally through the corals' lifespan with Re values increasing in the mid to late 19th century. The x-axis (year AD) was converted from radial distance (i.e., distance from center to outer edge) to year using radiocarbon derived growth rates between 8 and 22 µm yr^{-1} [*Prouty et al.*, 2011]. Superimposed on the concentration maps are the bulk nitrogen isotope (δ15N) time series from discrete sampling for isotopic variability from three individual coral specimens: (a) GOM-JSL09-3728-BC1, (b) GOM-JSL05-4876-BC1, and (c) GOM-TOW-BC2, and compound specific amino-acid (phenylalanine) nitrogen isotopes (δ15NPhe; inverted grey triangles) for GOM-JSL09-3728-BC1.

Oceans (e.g., *Fucus vesiculous*, *Macrocystisintegrifolia*, *and Pelvetia fastigiata*), which report Re concentrations between 4 and 80 ppb [*Scadden*, 1969; *Yang*, 1991; *Mas et al.*, 2005].

Rhenium concentrations from the upper 2 cm of 10 individual sediment tube cores range between 1.4 and 7.3 ppb, with an average value of 3.7 ± 2.1 ppb. The range in sediment Re values is consistent with the Re values measured in the sediment trap samples, 1.4 to 2.7 ppb (Table 3). These Re values are slightly elevated relative to the crustal abundance of Re, 0.5 to 1 ppb [*Greenwood and Earnshaw*, 1997], but not enriched enough to suggest an authigenic source [*Morford et al.*, 2005].

On average, the bituminous coal samples yielded a Re concentration of 3.1 ppb, with anthracite yielding the highest Re concentration, 6.7 ppb, and the lignite sample yielding the lowest Re concentration, 0.70 ppb

Table 2. Key Parameters Used to Calculate the Concentration Factor (CF), Pre-Anthropogenic Freshwater and Seawater Re Values, and Anthropogenic Re Contribution (%) to Present-day Riverine Concentrations

Parameter	Value
Average freshwater end-member [Re][a]	16.5 ppt
Average seawater end-member [Re][a]	8.3 ppt
Coral Re (post 1850)	8–9 ppm
Coral Re (pre 1850)	4 ppm
Concentration factor	10^6
Pre-anthropogenic seawater end-member [Re]	3.9 ppt
Pre-anthropogenic freshwater end-member [Re]	10.8 ppt
Conservative mixing line slope	-2×10^{-7}
Change in freshwater end-member [Re]	5.7 ppt
Anthropogenic contribution (%)	34%

[a][*Miller et al.*, 2011; *Shim et al.*, 2012].

(Figure 8). Coal grades with greater percent carbon also showed greater Re concentrations. The range of Re concentrations in the coal samples is consistent with the range of Re concentration in mine waters (2.2–6.9 ppb) [*Miller et al.*, 2011], with the exception of the lignite sample that was below the reported range (Figure 8).

3.3. Isotopes

Coral skeleton δ^{15}N values (10.88 to 11.68‰) are within the range measured for tissue δ^{15}N values (9.51 to 12.54‰), consistent with previous reports for gorgonian corals where no δ^{15}N fractionation existed between the tissue and skeleton [*Heikoop et al.* 2002; *Sherwood et al.*, 2005]. In comparison, the average δ^{15}N of suspended POM in the northern Gulf of Mexico is between 3.5 and 3.8 ± 0.7‰ [*Demopoulos et al.*, 2010], within the δ^{15}N range of nitrate (3.4 and 6.4‰) [*Battaglin et al.*, 2001] and average sediment trap δ^{15}N values (4.2‰) [*Mienis et al.*, 2012], but depleted relative to the coral skeleton and tissue as predicted from trophic enrichment. The tropic level was calculated at a position of 2, as defined by $TP_{Glu/Phe}$ [*Chikaraishi et al.*, 2009]. Assuming 3‰ enrichment per trophic level in bulk δ^{15}N [*DeNiro and Epstein*, 1981], this would yield a coral skeleton and coral tissue value of 6‰ greater than the source. With the source material yielding a δ^{15}N signature of between 4 and 7‰ [*Mienis et al.*, 2012], a 6‰ enrichment (11 to 13‰) is consistent to what we measure in the coral skeleton and coral tissue. The mean δ^{13}C value from black coral tissue samples ($n = 16$), −19.23 ± 0.76‰, is consistent with average δ^{13}C of surface POM in the northern Gulf of Mexico, −20 to −19.8 ± 0.8‰ [*Demopoulos et al.*, 2010].

Compound-specific amino acid δ^{15}N values separate into two groups (Figure 9) with Trophic-AA (Tr-AA) enriched in δ^{15}N as a function of isotopic fractionation during metabolic processes, versus the Source-AA (Sr-AA) which are relatively stable but affected by changes in source nutrients [*McClelland and Montoya*, 2002; *Chikaraishi et al.*, 2009]. The $\delta^{15}N_{Phe}$ values from 1970 to 2000 are relatively stable, varying between 9.7 and 11.7‰ (Figure 10). In contrast, pre-anthropogenic $\delta^{15}N_{Phe}$ values average 5.3‰, representing a statistically significant (Welch t test, $p < 0.05$) shift of 4.4‰ between the modern and pre-anthropogenic samples, which parallels the increase measured in bulk δ^{15}N values (Figure 10). This shift parallels the distinct increase in bulk-δ^{15}N values in the most recent period of skeletal growth (between 1000 and 675 μm), which is coupled to the Re increase described above (Figure 6). The relatively abrupt δ^{15}N increase observed over the last 150–200 years represents a baseline shift of between 1 and 3‰. The δ^{15}N rise occurs in the 1920s in the Viosca Knoll region and approximately 20 years earlier in the De Soto Canyon region. In contrast, there was no significant change in trophic position, as defined by $TP_{Glu/Phe}$ [*Chikaraishi et al.*, 2009], over the last two millennia (Figure 10).

4. Discussion

As sessile benthic suspension feeders, proteinaceous corals (including black corals) feed on rapidly exported, photosynthetically derived particulate organic matter [*Sherwood et al.*, 2011], as confirmed by stable isotopic analyses. The black corals are most likely feeding on a mixture of surface derived zooplankton and phytoplankton, consistent with a higher trophic level of Antipatharia [*Sherwood et al.*, 2008]. The presence of bomb-derived ^{14}C in the outermost samples of those corals collected alive confirms that sinking POM is the dominant carbon source to the deep-sea corals [*Prouty et al.*, 2011]. The exact pathway for coral Re uptake and bioaccumulation remains unclear, but likely represents a combination of dissolved-phase exposure through adsorption of Re in seawater and

Table 3. Inventory of Rhenium (Re) Concentrations From a Select Suite of Biological Samples and Sediment Samples

Sample	Range [Re]	Average [Re]
POM ($n = 6$)	0.005–1.6 ppt	0.3 ± 0.63 ppt
Zooplankton ($n = 11$)	0.2–1.4 ppt	0.7 ± 0.38 ppt
Sediment (trap) ($n = 11$)	1.4–2.7 ppb	1.95 ± 0.36 ppb
Sediment (core) ($n = 10$)	1.4–7.3 ppb	3.7 ± 2.1 ppb
Sargassum sp. ($n = 11$)	0.08–1.1 ppb	0.30 ± 0.35 ppb

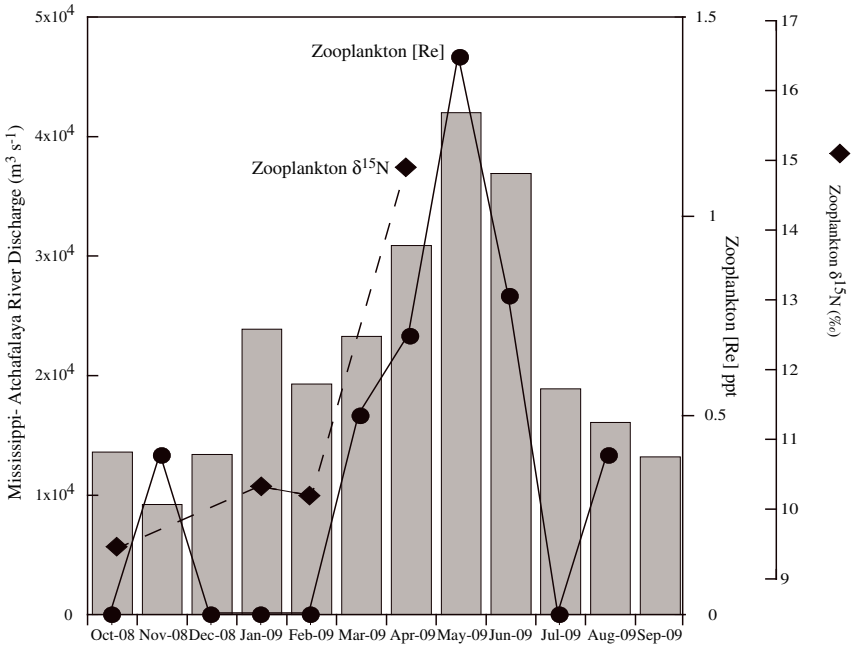

Figure 7. Monthly zooplankton rhenium (Re) concentration (ppt) and nitrogen isotope (δ15N) (‰) derived from monthly sediment trap samples deployed at Viosca Knoll from October 2008 to September 2009 compared to average Mississippi-Atchafalaya River discharge (m^3 s^{-1}) for the same time period [*Aulenbach et al.*, 2007]. Zooplankton Re detection limit was 0.2 ppt and samples with Re concentration below detection are plotted as zero concentration and available δ15N values are plotted for Oct., Jan., Feb., and Apr. from 2008 to 2009.

particulate-phase source associated with ingested food via the trophic web. Rhenium from hydrothermal fluid sources is negligible [*Miller et al.*, 2011], and Re from sediment resuspension is unlikely given the elemental distribution of Re is consistent with the Mississippi River outflow system, with Re concentrations inversely proportional to salinity [*Miller et al.*, 2011, *Shim et al.*, 2012], rather than an authigenic source. Our results also

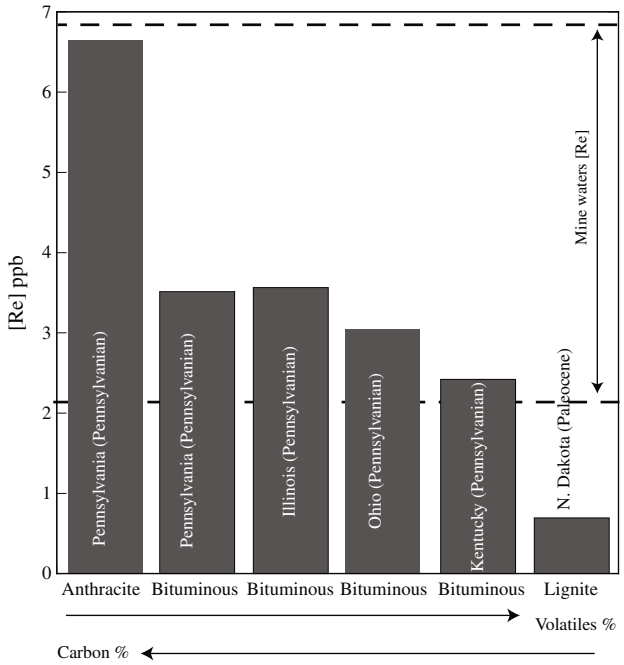

Figure 8. Rhenium (Re) concentrations (ppb) from a suite of coal samples collected from the coalfields of the Interior and Gulf Provinces (Figure 1), including samples of anthracite, bituminous, and lignite coal and their respective percent carbon and volatiles. For comparison, the range of Re concentrations measured in mine water samples is shown [*Miller et al.*, 2011].

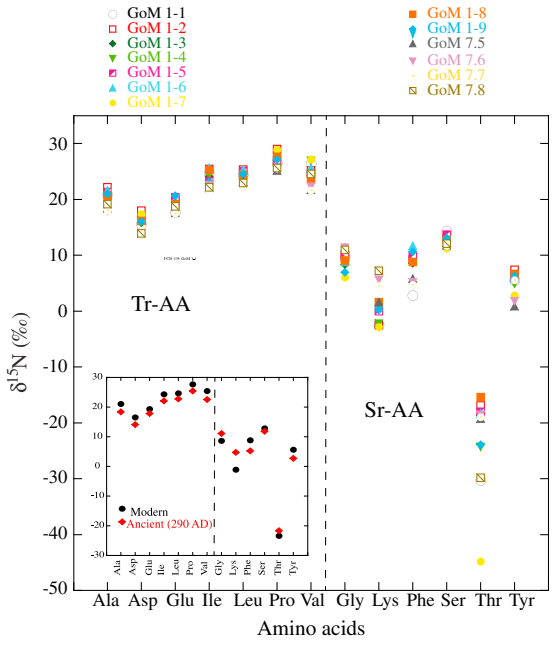

Figure 9. Compound specific amino-acid (δ15N-AA) distribution from 13 discrete black coral growth layers from the black coral sample GOM-JSL09-3728-BC1. Dashed line indicates separation between Trophic-AA (Tr-AA) and Source-AA (Sr-AA) with the Tr-AA demonstrating δ15N enrichment with trophic transfer. Average δ15N-AA values from the modern growth layers and premodern samples, centered at a calibrated radiocarbon age of 290 AD, are plotted in inset.

confirm that coral uptake of Re is in the form of perrhenate, the form also found in oxygenated natural waters and highly mobile in biogeochemical cycles [*Tagami and Uchida*, 2008], and therefore easily transported by rivers [*Miller et al*., 2011]. Analysis of monthly sediment trap zooplankton Re values from the study region strongly supports this view, suggesting a direct temporal link between biogenic Re input and Mississippi-Atchafalaya River outflow. Zooplankton Re values peak in May 2009, coincident with the peak in average Mississippi-Atchafalaya River discharge in 2009 (Figure 7). Zooplankton $\delta^{15}N$ values also peak in April, following the zooplankton Re enrichment during the onset of peak discharge. Taken together, these data clearly indicate that Re in deep-sea corals is derived from surface-derived sources that are also tightly coupled to Mississippi River discharge.

The striking increase in Re concentration observed in the black coral concentration maps, and the timing of the increase over the last two centuries, implicates anthropogenic forcing as the primary driver of Re variability in the most recent century. Anthropogenic activity since the industrial revolution (e.g., fossil fuel combustion, mining, and biomass burning) has had a significant impact on mobilization of metals and other elements, particularly Re [*Klee and Graedel*, 2004]. This observation is consistent with a mass balance calculation where the anthropogenic contribution to riverine Re (2.8×10^6 g Re) is equivalent to the calculated mass of Re produced from coal production, 3.0×10^6 g (Table 4). The increase we observe in coral Re values parallels the spread of coal mining in the 19th century and the increase in production of bituminous coal since the 1870s (Figure 11), linking recent Re values to anthropogenic sources, particularly those associated with coal combustion activities and enriched Re measured in coal samples (Figure 8). Because of its high mobility, Re released to the environment can be easily leached, weathered from surface sediment, and transported by rivers, serving as the major source of seawater Re [*Miller et al*., 2011]. The Mississippi River and associated watershed encompasses the major US coal producing regions (Figure 1) and is thus a natural conduit for Re flux to the Gulf of Mexico, with Mississippi River Re concentrations enriched 40 times greater than the global average [*Rahaman and Singh*, 2010].

According to a calculated CF of 10^6 and the slope of the conservative mixing line, pre-anthropogenic freshwater end-member Re value was approximately 10.8 ppt, yielding an anthropogenic contribution of approximately 34% to present-day Mississippi River Re concentrations (Table 2). These results provide the first independent calculation addressing earlier attempts to calculate an anthropogenic contribution [*Miller et al*., 2011] and the first ever biogenic archive of both natural and anthropogenic Re variability. Finally, given the tight coupling of the Re and C_{org} cycles [*Dalai et al*., 2002], the pre-anthropogenic riverine Re calculation described above can be used to estimate the release of CO_2 from chemical weathering of organic-rich sediment. The influence of weathering of organic-rich sediment on the flux of CO_2 prior to anthropogenic contribution of Re was calculated by estimating the flux of Re (mmol km^{-2} yr^{-1}) and applying a molar Re/C_{org} ratio of 7×10^{-8} [*Jaffe et al*., 2002]. With a pre-anthropogenic riverine Re concentration of 10.8 ppt, estimated from the coral record (Table 2), and assuming a watershed drainage area of 3.27×10^6 km^2 [*Graham et al*., 1999], weathering of organic-rich sediment would release 1.9×10^5 moles CO_2 km^{-2} yr^{-1} (Table 4). This is equivalent to releasing 7.4×10^{12} g C yr^{-1}, consistent with previous estimates of the CO_2 flux from the Mississippi River tributaries, 7.8×10^{12} g C yr^{-1} [*Dubois et al*., 2010].

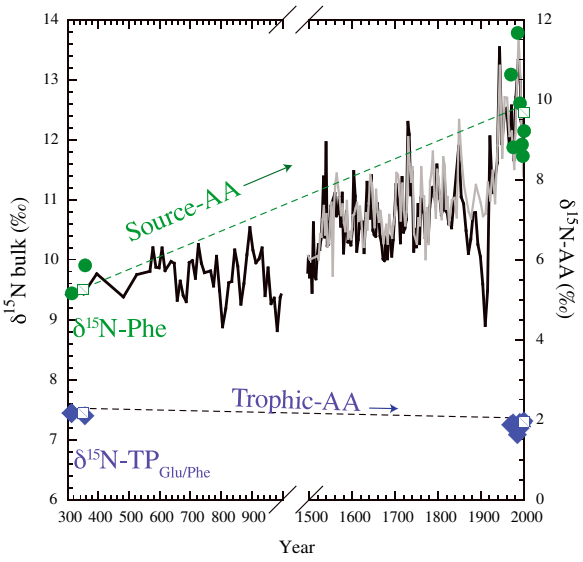

Figure 10. Discrete compound specific amino-acid (phenylalanine) nitrogen isotopes ($\delta^{15}N_{Phe}$) from 10 individual growth layers (green circles) superimposed on the $\delta^{15}N$ bulk record (black line) from 300 to 2000 AD from the coral specimen GOM-JSL09-3728-BC1. The $\delta^{15}N$ bulk time series was replicated on a different radial transect (grey line) over the outer 7 mm (approximately 880 years). The $\delta^{15}N_{Phe}$ increase of 4.4‰ tracks the bulk $\delta^{15}N$ enrichment through the lifespan of the coral. There was no significant change in trophic position, as defined by $TP_{Glu/Phe}$ (blue diamonds). Dashed lines connect the modern and ancient $\delta^{15}N_{Phe}$ (green) and $\delta^{15}N_{TP}$ (blue) average values.

With enhanced chemical weathering predicted as a result of climate and land use changes [*Beaulieu et al.*, 2012], there is a strong potential for this estimate to increase, leading to enhanced fluxes in riverine bicarbonate [*Raymond et al.*, 2008].

The dramatic Re increase we observe is also coupled to an enriched bulk $\delta^{15}N$ signal in the most recent period of coral skeletal growth (Figure 6). The $\delta^{15}N$ increase begins in the 1920s in the Viosca Knoll region and approximately 20–30 years earlier in the De Soto Canyon region. This offset between the two sites may be related to a change in the course of the Mississippi River. In 1876 the Mississippi River cut across De Soto Peninsula, breaking the De Soto Point and therefore altering its outflow pattern. The abrupt $\delta^{15}N$ increase of 3–4‰ we measured in the coral record in the late 1800s also parallels the increase in land drainage in the Mississippi River Basin and the ensuing increase in nitrate flux in the Mississippi River [*Mitsch et al.*, 2001], suggesting that similar anthropogenic activities linked to Re increases have also profoundly altered the N biogeochemistry in the Gulf of Mexico.

However, changes in bulk $\delta^{15}N$ values alone are ambiguous because they could reflect shifts in the $\delta^{15}N$ of source N at the base of the food web, broad changes in food-web trophic structure, or some combination of both. However, results from $\delta^{15}N$-AA analysis delineate the relative influence of possible nitrogen source $\delta^{15}N$ changes versus potential trophic structure changes [*McClelland and Montoya*, 2002; *McCarthy et al.*, 2007] underlying the large shifts in bulk $\delta^{15}N$. As a proxy of source N given the little change in $\delta^{15}N$ with each trophic level [*McClelland and Montoya*, 2002; *Chikaraishi et al.*, 2009], $\delta^{15}N_{Phe}$ values can be used as a direct tracer for $\delta^{15}N$ changes at the base of the food web [*Sherwood et al.*, 2011]. The $\delta^{15}N_{Phe}$ values from 1970 to 2000 are relatively stable, varying between 9.7 and 11.7‰. In contrast, pre-anthropogenic $\delta^{15}N_{Phe}$ values average 5.3‰, representing a shift of 4.4‰ between the modern and pre-anthropogenic samples, which parallels the increase measured in bulk $\delta^{15}N$ values. In contrast, there was no significant change in trophic position, as defined by $TP_{Glu/Phe}$ [*Chikaraishi et al.*, 2009] (Figure 10). Together, the strong linkage between $\delta^{15}N_{Phe}$ and bulk $\delta^{15}N$ values, coupled with lack of change in trophic position over the much longer coral record, indicates that the recent increase in bulk $\delta^{15}N$ values is due to rapid changes in inorganic nitrogen $\delta^{15}N$ values in the Gulf of Mexico.

Table 4. Watershed Parameters Used to Calculate Re Flux mmoles km^{-2} yr^{-1} and Release of CO_2 moles km^{-2} yr^{-1} and C g yr^{-1}

Parameter	Value
Re/C_{org}[a]	7×10^{-8}
Mississippi River Watershed area (km^2)[b]	3,270,000
Mississippi River discharge (L yr^{-1})[c]	5.3×10^{14}
Re flux (mmoles km^{-2} yr^{-1})	9.4
CO_2 flux (moles km^{-2} yr^{-1})	1.9×10^5
C flux (g yr^{-1})	7.4×10^{12}

[a][*Jaffe et al.*, 2002].
[b][*Graham et al.*, 1999].
[c][*Kammerer*, 1987].

With 58% of the river basin devoted to agricultural land, the primary source of nitrogen to the Mississippi River is from fertilizer use [*Battaglin et al.*, 2001], which has been shown to enhance nitrate leaching [*Donner and Foley*, 2004]. While synthetic fertilizer nitrogen $\delta^{15}N$ values are low, nitrogen derived from manure or human waste typically has elevated $\delta^{15}N$ values [*Heaton*, 1986]. In addition, in anoxic environments such as the northern Gulf of Mexico, denitrification can also cause the $\delta^{15}N$ of the residual nitrate to increase [*Kendall et al.*, 2007]; denitrification rates have been increasing with increased

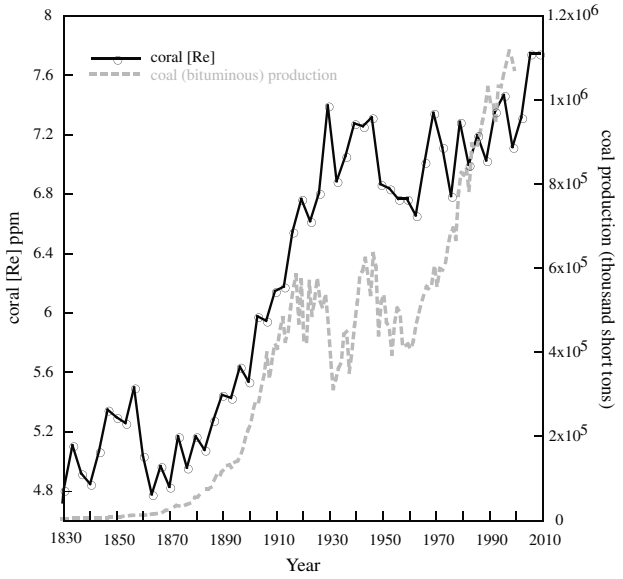

Figure 11. Coral rhenium (Re) variability (ppb) from 1830 to 2009 (GOM-JSL09-3728-BC1) compared to the increase in US coal production of bituminous coal in thousands short tons [*Carter et al*., 2006] illustrating the concomitant rise in coal production and Re concentration in the late 19th century. Coral Re time series represents the average of 20 scans across a radial transect spaced ~40 μm apart.

nitrogen loading [*Kellman and Hillaire-Marcel*, 1998]. The average sediment trap $\delta^{15}N$ values (4.2‰) [*Mienis et al*., 2012] are well within the $\delta^{15}N$ range reported for Mississippi River nitrate (3.4 to 6.4‰) [*Battaglin et al*., 2001]. Given that nitrate dominates the Mississippi River dissolved inorganic nitrogen pool [*Kendall et al*., 2001], these deep-sea corals are almost certainly capturing the increase in riverine nitrate flux that has been well documented in the Gulf of Mexico [*McIsaac et al*., 2001; *Battaglin et al*., 2001]. Therefore both primary (e.g., nitrogen source) and secondary (e.g., denitrification) impacts of nitrogen loading are being captured in the coral skeletal bulk-$\delta^{15}N$ and $\delta^{15}N$-AA records.

The linked increases in coral bulk $\delta^{15}N$, $\delta^{15}N_{Phe}$, and Re values tell us that with the onset of agro-industrialization and an increase in the intensity of land use change (e.g., tile drainage, fertilizer use, tillage, and irrigation) in the Mississippi River watershed over the last 200 years, nutrient overenrichment in adjacent coastal ecosystems has fundamentally shifted the biogeochemistry of the deep-sea ecosystem in the Gulf of Mexico. Continued export of nitrogen, carbon, sediment, and associated pollutants to the Gulf of Mexico is predicted to accelerate with climate change as precipitation and runoff increase in the upper part of the Mississippi River watershed [*Milliman et al*., 2008; *Raymond et al*., 2008; *Beaulieu et al*., 2012]. Conservation goals by the Mississippi River/Gulf of Mexico Watershed Nutrient Task Force include reduction in fertilizer use, nitrate transport, and contaminants through modifying agricultural practices [*Mitsch et al*., 2001]. Without baseline information, however, these targets remain elusive, especially if response times of the marine system are unknown. Results from these novel tracers provide important baseline information about trace metals and nutrients that can help inform efforts to reduce future fertilizer use, nitrate transport, and watershed restoration.

5. Conclusion

Our coupled analysis of trace metals, bulk $\delta^{15}N$, and $\delta^{15}N$-AA in corals from the Gulf of Mexico capture the rapid sensitivity of deep-sea corals to upstream changes in watershed quality, providing not only a temporal perspective over the last millennia, but also a quantitative context to evaluate effects of future and ongoing land use and climate change on nutrient loading and downstream biogeochemical cycles. As a first record of pre-industrial Re variability, these novel records also quantify the anthropogenic contribution of Re in the Mississippi River and to the Gulf of Mexico, thereby constraining the relationship between riverine Re flux and CO_2 inventory through land use change. The unequivocal increase in nitrogen source values captured in

these corals further links anthropogenic activities to the apparent profound alteration of the N biogeochemistry in the Gulf of Mexico, demonstrated by the rapid shift in baseline nitrogen isotope values. Additional changes caused by land use change, such as hypoxia and alteration of food-web structure, are not unique to the Gulf of Mexico. The ubiquitous distribution of deep-sea corals, coupled with this new tracer suite, therefore provides a highly sensitive new approach to understand the downstream effects of human activity on coastal waters and less well-studied marine deep-water ecosystems.

Acknowledgments
The USGS Terrestrial, Marine, and Freshwater Environments-Outer Continental Shelf Ecosystem Program and USGS Coastal and Marine Geology Program and a grant to EBR from The Norman Hackerman Advanced Research Program supported this work. We thank P. Lamothe, R. Wolf, and T. Todorov (USGS) for assistance with trace metal analysis, and J. McClain-Counts (USGS), M. Sutor (LSU), and J. Rooker (Texas A&M) for providing sediment, POM, and algae samples, B. Williams (Claremont) for archived sample identification, J. Kirk for providing preliminary coal data, S. Ross (UNC-Wilmington), K. Sulak (USGS), and S. Cairns (Smithsonian Institution National Museum of Natural History) for donating samples, D. Opresko for species identification of samples, and P. Swarzenski and M. Foley (USGS) for helpful discussion.

References

Aulenbach, B. T., H. T. Buxton, W. T. Battaglin, and R. H. Coupe (2007), Streamflow and nutrient fluxes of the Mississippi-Atchafalaya River Basin and subbasins for the period of record through 2005, *U.S. Geological Survey Open-File Report 2007–1080*.

Baker, D. M., K. L. Webster, and K. Kim (2010), Caribbean octocorals record changing carbon and nitrogen sources from 1862 to 2005, *Global Change Biol*, *16*, 2701–2710.

Battaglin, W. A., K. C. Kendall, C. C. Y. Chang, S. R. Silva, and D. H. Campbell (2001), Chemical and isotopic evidence of nitrogen transformation in the Mississippi River, 1997–98, *Hydrol. Processes*, *15*, 1285–1300.

Beaulieu, E., Y. Goddéris, Y. Donnadieu, D. Labat, and C. Roelandt (2012), High sensitivity of the continental-weathering carbon dioxide sink to future climate change, *Nat. Clim. Change*, *2*, 346–349, doi:10.1038/nclimate1419.

Carter, S. B., S. Gartner, M. Haines, A. Olmstead, R. Sutch, and G. Wright (2006), *Historical Statistics of the United States: Earliest Times to the Present, Part C: Economic Structure and Performance*, pp. 861, Cambridge Univ. Press, New York.

Chikaraishi, Y., N. O. Ogawa, Y. Kashiyama, Y. Takano, H. Suga, A. Tomitani, H. Miyashita, and N. Ohkouchi (2009), Determination of aquatic food-web structure based on compound- specific nitrogen isotopic composition of amino acids, *Limnol. Oceanogr. Methods*, *7*, 740–750.

Colodner, D., J. Sachs, G. Ravizza, K. Turekian, J. Edmond, and E. Boyle (1993), The geochemical cycle of rhenium: A reconnaissance, *Earth Planet. Sci. Lett.*, *117*, 205–221.

Crusius, J., S. Calvert, T. Pedersen, and D. Sage (1996), Rhenium and molybdenum enrichments in sediments as indicators of oxic, suboxic, and sulfidic conditions of deposition, *Earth Planet. Sci. Lett.*, *145*, 65–78.

CSA International (2007), Characterization of Northern Gulf of Mexico deepwater hard bottom communities with emphasis on Lophelia coral, in *OCS Study MMS 2007–044 Minerals Management Service*, edited by US Department of Interior, 169 pp., Gulf of Mexico OCS Region, New Orleans, La.

Dalai, T. K., S. J. Singh, J. R. Trivedi, and S. Krishnashwami (2002), Dissolved rhenium in the Yamuna river system and the Ganga in the Himalaya: Role of black shale weathering on the budgets of Re, Os, and U in rivers and CO_2 in the atmosphere, *Geochim. Cosmochim. Acta*, *66*, 29–43.

Davies, A. J., G. C. A. Duineveld, T. C. E. van Weering, F. Mienis, A. M. Quattrini, H. E. Seim, J. M. Bane, and S. W. Ross (2010), Short-term environmental variability in cold-water coral habitat at Viosca Knoll, Gulf of Mexico, *Deep Sea Res., Part I*, *57*, 199–212.

Demopoulos, A. W. J., D. Gualtieri, and K. Kovacs (2010), Food-web structure of seep sediment macrobenthos from the Gulf of Mexico, *Deep Sea Res., Part II*, *57*, 1972–1981, doi:10.1016/j.dsr2.2010.05.011.

Deniro, M. J., and S. Epstein (1981), Influence of diet on the distribution of nitrogen isotopes in animals, *Geochim. Cosmochim. Acta*, *45*(3), 341–351.

Donner, S. D., and J. A. Foley (2004), The impact of changing land use practices on nitrate export by the Mississippi Basin, *Global Biogeochem. Cycles*, *18*, GB1028, doi:10.1029/2003GB002093.

Dubois, K. D., D. Lee, and J. Veizer (2010), Isotopic constraints on alkalinity, dissolved organic carbon, and atmospheric carbon dioxide fluxes in the Mississippi River, *J. Geophys. Res.*, *115*, G02018, doi: 10.1029/2009JG001102.

Goldberg, W. M. (1991), Chemistry and structure of skeletal growth rings in the black coral *Antipathes fiordensis* (Cnidaria, Antipathatia), *Hydrobiologia*, *216*, 403–409.

Graham, S. T., J. S. Famiglietti, and D. R. Maidment (1999), Five-minute, 1/2°, and 1° data sets of continental watersheds and river networks for use in regional and global hydrologic and climate system modeling studies, *Water Resour. Res,*. *35*, 583–587.

Greenwood, N. N., and A. Earnshaw (1997), *Chemistry of the Elements*, 2nd ed., pp. 340, Butterworth-Heinemann, Oxford, U. K.

Heaton, T. H. E. (1986), Isotopic studies of nitrogen pollution in the hydrosphere and atmosphere: A review, *Chem. Geol.*, *5*, 87–102.

Heikoop, J. M., D. D. Hickmott, M. J. Risk, C. K. Shearer, and V. Atudorei (2002), Potential climate signals from the deep-sea gorgonian coral *Primnoa resedaeformis*, *Hydrobiologia*, *471*, 117–124.

Jaffe, L. A., B. Peucker-Ehrenbrink, and S. T. Petsch (2002), Mobility of rhenium, platinum group elements and organic carbon during black shale weathering, *Earth Planet. Sci. Lett.*, *198*, 339–353.

Kammerer, J. C. (1987), Largest Rivers in the United States. US Geological Survey Fact Sheet *OFR 87–242* rev. 1990.

Kellman, L., and C. Hillaire-Marcel (1998), Nitrate cycling in streams: Using natural abundances of NO_3^- – $\delta^{15}N$ to measure in situ denitrification, *Biogeochemistry*, *43*, 273–292.

Kendall, C., R. S. Steven, and V. J. Kelly (2001), Carbon and nitrogen isotopic compositions of particulate organic matter in four large river systems across the United States, *Hydrol Process*, *15*, 1301–1346.

Kendall, C., E. M. Elliott, and S. D. Wankel (2007), Tracing anthropogenic inputs of nitrogen to ecosystems, chap. 12, in *Stable Isotopes in Ecology and Environmental Science*, 2nd ed., edited by R. H. Michener and K. Lajtha, pp. 375–449, Blackwell Publishing, Oxford, U. K.

Kirk, J., J. Ruiz, J. Chesley, J. Walshe, and G. England (2002), A major Archean, gold- and crust-forming event in the Kaapval craton South Africa, *Science*, *297*, 1856–1858.

Klee, R. J., and T. E. Graedel (2004), Elemental cycles: A status report on human or natural dominance, *Annu. Rev. Environ. Resour.*, *29*, 69–107.

Koenig, A. E., R. A. Roger, and C. N. Trueman (2009), Visualizing fossilization using laser-ablation inductively coupled plasma-mass spectrometry maps of trace elements in Late Cretaceous bones, *Geology*, *37*, 511–514.

Longerich, H. P., S. E. Jackson, and D. Günther (1996), Laser ablation inductively coupled plasma mass spectrometric transient signal data acquisition and analyze concentration calculation, *J. Anal. Atom. Spectrom.*, *11*, 899–904.

Mas, J. L., K. Tagami, and S. Uchida (2005), Rhenium measurements on North Atlantic seaweed samples by ID-ICP-MS: An observation on the Re concentration factors, *J. Radioanal Nucl Ch.*, *265*, 361–365.

McCarthy, M., R. Benner, C. Lee, and M. Fogel (2007), Amino acid nitrogen isotopic fractionation patterns as indicators of heterotrophy in plankton, particulate, and dissolved organic matter, *Geochim. Cosmochim. Acta*, *71*, 4727–4744.

McClelland, J. W., and J. P. Montoya (2002), Trophic relationships and the nitrogen isotopic composition of amino acids in plankton, *Ecology*, *83*, 2173–2180.
McIsaac, G. F., M. B. David, G. Z. Gertner, and D. A. Goolsby (2001), Nitrate flux to the Gulf of Mexico, *Nature*, *414*, 166–167.
Mienis, F., G. C. A. Duineveld, A. J. Davies, S. W. Ross, H. Seim, J. Bane, and T. C. E. van Werring (2012), The influence of near-bed hydrodynamic conditions on cold-water corals in the Viosca Knoll area, Gulf of Mexico, *Deep Sea Res., Part I*, *60*, 32–45.
Miller, C. A., B. Peucker-Ehrenbrink, B. D. Walker, and F. Marcantonio (2011), Re-assessing the surface cycling of molybdenum and rhenium, *Geochim. Cosmochim. Acta*, *75*, 7146–7179.
Milliman, J. D., K. L. Farnsworth, P. D. Jones, K. H. Xu, and L. C. Smith (2008), Climatic and anthropogenic factors affecting river discharge to the global ocean, 1951–2000, *Global Planet. Change*, *62*, 187–194.
Mitsch, W. J., J. W. Day, J. W. Gilliam, P. M. Groffman, D. L. Hey, G. W. Randall, and N. Wang (2001), Reducing nitrogen loading to the Gulf of Mexico from the Mississippi River Basin: Strategies to counter a persistent ecological problem, *BioScience*, *51*, 373–388.
Morel, F. M. M., and N. M. Price (2003), The biogeochemical cycles of trace metals in the oceans, *Science*, *300*, 944–947.
Morford, J. L., S. R. Emerson, E. J. Breckel, and S. H. Kim (2005), Diagenesis of oxyanions (V, U, Re, and Mo) in pore waters and sediments from a continental margin, *Geochim. Cosmochim. Acta*, *69*, 5021–5032.
Peucker-Ehrenbrink, B., and G. Ravizza (2000), The marine osmium isotope record, *Terra Nova*, *12*, 205–219.
Prouty, N. G., E. B. Roark, N. A. Buster, and S. W. Ross (2011), Growth-rate and age distribution of deep-sea black corals in the Gulf of Mexico, *Mar. Ecol. Prog. Ser.*, *423*, 101–115.
Rabalais, N. N., R. E. Turner, and W. J. Wiseman (2002), Hypoxia in the Gulf of Mexico, a.k.a. "The Dead Zone", *Annu. Rev. Ecol. Evol. Syst.*, *33*, 235–263.
Rahaman, W., and S. K. Singh (2010), Rhenium in rivers and estuaries of India: Sources, transport and behavior, *Mar. Chem.*, *118*, 1–10.
Rahaman, W., S. K. Singh, and A. D. Shukla (2012), Rhenium in Indian rivers: Sources, fluxes, and contribution to oceanic budget, *Geochem. Geophys. Geosyst.*, *13*, Q08019, doi:10.1029/2012GC004083.
Raymond, P. A., N. H. Oh, R. E. Turner, and W. Broussard (2008), Anthropogenically enhanced fluxes of water and carbon from the Mississippi River, *Nature*, *451*, 449–52.
Risk, M. J., O. A. Sherwood, R. Nairn, and C. Gibbons (2009), Tracking the record of sewage discharge off Jeddah, Saudi Arabia, since 1950, using stable isotope records from antipatharians, *Mar. Ecol. Prog. Ser.*, *397*, 219–226.
Roark, E. B., T. P. Guilderson, R. B. Dunbar, S. J. Fallon, and D. A. Mucciarone (2009), Extreme longevity in proteinaceous deep-sea corals, *Proc. Natl. Acad. Sci. U. S. A.*, *106*, 5204–5208.
Scadden, E. M. (1969), Rhenium, *Geochim. Cosmochim. Acta*, *33*, 633–637.
Schoener, A., and G. T. Rowe (1970), Pelagic Sargassum and its presence among the deep-sea benthos, *Deep-Sea Res*, *17*, 923–925.
Selby, D., and R. A. Creaser (2001), Re-Os Geochronology and systematics in solybdenite from the Endako Porphyry Molybdenum Deposit, British Columbia Canada, *Econ. Geol.*, *96*, 197–204.
Selby, D., and R. A. Creaser (2005), Direct radiometric dating of the Devonian-Mississippian time-scale boundary using the Re-Os black shale geochronometer, *Geology*, *33*(7), 545–548.
Sherwood, O. A., J. M. Heikoop, D. B. Scott, M. J. Risk, T. P. Guilderson, and R. A. McKinney (2005), Stable isotopic composition of deep-sea gorgonian corals *Primnoa* spp: A new archive of surface processes, *Mar. Ecol. Prog. Ser.*, *301*, 135–148.
Sherwood, O. A., R. E. Jamieson, E. N. Edinger, and V. E. Wareham (2008), Stable C and N isotopic composition of cold-water corals from the Newfoundland and Labrador continental slope: Examination of trophic, depth and spatial effects, *Deep Sea Res., Part I*, *10*, 1392–1402.
Sherwood, O. A., B. E. Lapointe, M. J. Risk, and R. E. Jamieson (2010), Nitrogen isotopic records of terrestrial pollution encoded in Floridian and Bahamian gorgonian corals, *Environ. Sci. Technol.*, *44*, 874–880.
Sherwood, O., M. Lehmann, C. Schubert, D. Scott, and M. McCarthy (2011), Nutrient regime shift in the western North Atlantic indicated by compound-specific δ^{15}N of deep-sea gorgonian corals, *Proc. Natl. Acad. Sci. U. S. A.*, *108*, 1011–1015, doi:10.1073/pnas.1004904108.
Shim, M. J., P. W. Swarzenski, and A. M. Shiller (2012), Dissolved and colloidal trace elements in the Mississippi River Delta outflow after Hurricanes Katrina and Rita, *Cont. Shelf Res.*, *42*, 1–9.
Sulak, K. J., M. T. Randall, K. E. Luke, A. D. Norem, and J. M. Miller (2008), Characterization of Northern Gulf of Mexico deepwater hard bottom communities with emphasis on *Lophelia* coral - *Lophelia* reef megafaunal community structure, biotopes, genetics, microbial ecology, and geology, *USGS Open-File Report 2008–1148, OCS Study MMS 2008–015*.
Tagami, K., and S. Uchida (2008), Determination of bioavailable rhenium fraction in agricultural soils, *J. Environ. Radioact.*, *99*, 973–80.
Wakoff, B., and K. L. Nagy (2004), Perrhenate uptake by iron and aluminum oxyhydroxides: An analogue for pertechnetate incorporation in Hanford waste tank sludges, *Environ. Sci. Technol.*, *38*, 1765–1771.
Williams, B., and A. G. Grottoli (2010a), Stable nitrogen and carbon isotope (δ^{15}N and δ^{13}C) variability in shallow tropical Pacific soft coral and black coral taxa and implications for paleoceanographic reconstructions, *Geochim. Cosmochim. Acta*, *74*, 5280–5288.
Williams B., and A. G. Grottoli (2010b) Recent shoaling of the nutricline and thermocline in the western tropical Pacific, *Geophys Res Lett*, *37*, L22601, doi:10.1029/2010GL044867.
Williams, B., M. J. Risk, S. W. Ross, and K. J. Sulak (2006), Deep-water antipatharians: Proxies of environmental change, *Geology*, *34*, 773–776.
Williams, B., M. J. Risk, S. W. Ross, and K. J. Sulak (2007), Stable isotope data from deep-water Antipatharians: 400-year records from the southeastern coast of the United States of America, *Bull. Mar. Sci.*, *81*, 437–447.
Yang, J. S. (1991), High rhenium enrichment in brown algae, *Hydrobiologia*, *211*, 165–170.

Erratum

In the originally published version of this article, Steve W. Ross was not included in the author list. The authorship has since been corrected and this version may be considered the authoritative version of record.